

From Brueckner approach to Skyrme-type energy density functional

L. G. Cao,¹ U. Lombardo,^{1,2} C. W. Shen,³ and Nguyen Van Giai⁴

¹*Laboratori Nazionali del Sud, INFN, Via Santa Sofia 44, I-95123 Catania, Italy*

²*Dipartimento di Fisica dell'Università, Viale Andrea Doria 6, I-95123 Catania, Italy*

³*School of Science, Huzhou Teachers College, No. 1 Xueshi Road, Huzhou 313000, China*

⁴*Institut de Physique Nucléaire, Université Paris Sud, F-91406 Orsay CEDEX, France*

(Received 27 July 2005; published 26 January 2006)

A Skyrme-like effective interaction is built up from the equation of state of nuclear matter. The latter is calculated in the framework of the Brueckner-Hartree-Fock approximation with two- and three-body forces. A complete Skyrme parametrization requires a fit of the neutron and proton effective masses and the Landau parameters. The new parametrization is probed on the properties of a set of closed-shell and closed-subshell nuclei, including binding energies and charge radii.

DOI: [10.1103/PhysRevC.73.014313](https://doi.org/10.1103/PhysRevC.73.014313)

PACS number(s): 21.30.Fe, 21.60.Jz, 21.65.+f, 21.10.Dr

I. INTRODUCTION

For more than 30 years, the microscopic description of nuclear ground state properties is relying on the self-consistent mean field approach, or Hartree-Fock (HF) approach built from effective in-medium nucleon-nucleon interactions [1]. The most popular interaction is the Skyrme-type interaction [2], whose analytic form leads to considerable simplification of the HF calculations in finite nuclei. The general point of view is that the Skyrme interaction is a phenomenological one whose parameters are directly adjusted on a few selected observables taken from infinite matter and some doubly magic nuclei. In its most sophisticated versions, the Skyrme-type force can predict binding energies of all measured nuclei with an overall error of less than 0.7 MeV [3]. Other parametrizations try to improve the description of systems with a large neutron excess [4] by incorporating constraints from variational calculations performed for neutron-rich and pure neutron matter [5,6].

On the other hand, important progress has been made in recent years concerning Brueckner-Hartree-Fock (BHF) calculations of infinite matter [7,8]. For many years, a major drawback of the BHF approach was that the empirical saturation point of symmetric nuclear matter could not be reproduced if one starts with only a realistic two-body bare interaction (the so-called Coester line problem). This is why in the early attempts to derive from a Brueckner G matrix an effective interaction suitable for HF calculations of finite nuclei it was necessary to renormalize phenomenologically the G matrix [9,10]. Two recent achievements have taken the BHF approach to a quite satisfactory status: one is that the convergence of the hole-line expansion has been proved to occur already at the level of three-body correlations [7]; the other is that the inclusion of three-body forces improves to a large extent the prediction of the saturation point [8].

Thus, it is timely to reexamine how one can relate the BHF description of homogeneous matter to a HF description of finite nuclei. Our strategy is to look for a Skyrme-like parametrization adjusted so as to reproduce the BHF results calculated in symmetric nuclear matter and also spin and isospin polarized matter, then to examine the HF predictions of this parametrization in nuclei. In our approach, it is possible to

determine all the parameters of the force except the two-body spin-orbit parameter W_0 because this component of the force gives no contribution to homogeneous matter. This will remain an adjustable parameter when calculating finite nuclei, and its value is fixed on the $1p_{1/2}$ - $1p_{3/2}$ splitting in ^{16}O as it is usually done. Of course, the two-body Coulomb interaction has also to be added.

In a recent work, Baldo *et al.* [11] studied the relation between the Brueckner results in infinite matter and some of the Skyrme parameters, but the number of constraints used was insufficient to determine the velocity-dependent part of the Skyrme force, which is a very important part since it governs the effective mass behavior.

In this work, we start from the recent BHF calculations of Refs. [8,12] extended to spin and isospin polarized homogeneous matter. The paper is organized as follows: Sec. II gives a brief review of relevant BHF predictions. In Sec. III, we explain how the Skyrme parameters are determined. Sec. IV presents and discusses the HF results obtained for selected closed-shell nuclei. Concluding remarks are given in Sec. V.

II. REVIEW OF THE RELEVANT BHF PREDICTIONS

The Brueckner theory of nuclear matter was recently reviewed in Ref. [13]. In this theory, the correlation energy is cast as a hole-line expansion, where the bare interaction is replaced by the G matrix, which incorporates the short-range correlations. The BHF approximation is obtained by truncating the expansion at the two hole-line level. Roughly speaking, it amounts to the Hartree-Fock approximation, where the role of the phenomenological interaction is played by the G matrix.

For densities of nuclear matter around or below the saturation value, the BHF method is a quite good approximation. In that region in fact, we are allowed to neglect the three-body correlations, which give a small contribution when adopting the continuous choice for the auxiliary potential [7]. On the other hand, the BHF approximation embodies both the inert core pure BHF mean field and the core polarization term, the latter arising as rearrangement potential [12]. Thus, the main effects of the correlations on the effective mass will be taken

into account. The fit of the microscopic effective mass is a qualifying aspect of the present parametrization, since this quantity is one of the least well-constrained properties of the phenomenological Skyrme forces [14].

Let us briefly review the salient features of the BHF equation of state (EOS):

(i) *Saturation point.* The BHF approach with only two-body forces sizeably overestimates the saturation density [13]. This is commonly attributed to the missing effect of the three-body force in the region above the empirical saturation density. Including a three-body force in the calculations improves the saturation density without appreciable change of the corresponding energy. The most recent Brueckner calculations [8] estimated $\rho_0 \approx 0.18 \text{ fm}^{-3}$, still beyond the range of the empirical values of the central density of nuclei, and the energy $\frac{E}{A} \approx -14.8 \text{ MeV}$. The main effect of such a failure is expected to appear in the calculation of the neutron and proton density profiles.

(ii) *Effective mass.* The nucleon effective mass inside the medium is an outcome of the BHF approach, and as such, it must be reproduced by the equivalent Skyrme parametrization. It is related to the momentum dependence of the on-shell self-energy $\Sigma(\epsilon_k, k)$, where ϵ_k is the quasiparticle energy. It plays an important role not only in the theoretical description of the transport phenomena, including heavy-ion collision (HIC) simulations, but also for the level density of nuclei. Recently, the isospin splitting of the effective mass has been the subject of some debate since different approaches predict contradictory results [15–18]. In the framework of the Brueckner approach, it is possible to trace the isospin splitting of the effective mass back to properties of the bare nuclear interaction [15,19]. It turns out that the neutron effective mass is linearly increasing with the neutron excess while the proton effective mass is symmetrically decreasing. When embodying the neutron and proton effective masses in the fit, one may expect important isospin effects in the observables which are sensitive to the effective mass itself. It has been recently pointed out [20] that $m_n^* < m_p^*$ leads to the wrong energy dependence of the Lane potential [21]. Another dynamical observable very sensitive to the effective mass is the in-medium nucleon-nucleon cross section. Therefore, heavy-ion collisions involving neutron-rich systems could provide direct experimental evidence of the isospin splitting of the effective mass [22].

(iii) *Symmetry energy.* The symmetry energy $a_s(\rho)$ has stimulated a lot of interest for its relevance in HIC physics, nuclear astrophysics, and exotic nuclei. In fact, it is related to the isospin splitting of effective mass, neutron and proton mean fields, etc. In particular, the neutron skin in neutron-rich nuclei seems to be very sensitive to the details of the density dependence of $a_s(\rho)$ [23]. In the microscopic approaches, the saturation point becomes less and less stable with increasing neutron excess, and at some critical point, before reaching the conditions of pure neutron matter, it disappears. This transition formally amounts to the transition from a minimum to an inflection point in the function $\frac{E}{A}(\beta, \rho)$. Correspondingly the symmetry energy would also exhibit an inflection point as a function of density. This means that any parametrization of $a_s(\rho)$ such as ρ^α , which is often adopted in calculations, is not suitable for reproducing this behavior. This seems to be

the case with the Skyrme forces. In the BHF approximation, the symmetry energy at the saturation point turns out to be $a_s(\rho_0) \approx 34 \text{ MeV}$ [8]. At low density, it is independent of the force [11], and therefore it can be considered well established from the viewpoint of a quantum-mechanical many-body theory. Above the saturation point, the three-body force has a strong influence on the symmetry energy. The BHF prediction is in rather good agreement with the relativistic Dirac-Brueckner [16], but both diverge from variational calculations [5,6] and also from some Skyrme forces (for a discussion, see Ref. [14]). The structure of neutron stars has been addressed as a possible constraint for the EOS of asymmetric nuclear matter, particularly, for the symmetry energy, but so far the calculations do not give a definite answer.

(iv) *Landau parameters.* To have a full determination of the Skyrme force parameters and not only some combinations of them, it is not sufficient to fit bulk properties such as binding energies, effective masses, and symmetry energy, as we shall see in Sec. III. These properties are in fact related to only the time-even part of the BHF energy functional [24]. We will use the additional constraint of reproducing the G_0 Landau parameter extracted by extending the BHF calculations to spin and isospin polarized nuclear matter [25], which gives the time-odd part of the BHF energy functional.

The Brueckner predictions for the Landau parameters [25] have proved to reproduce the existing experimental data; in particular, the parameter G'_0 is consistent with the centroid energy of the Gamow-Teller giant resonance [26]. So far, only the values of the Landau parameters at the saturation point can be tested. At lower density, experimental information can come from the study of giant resonances in exotic nuclei.

III. DETERMINATION OF SKYRME FORCE PARAMETERS

The standard form of the Skyrme effective interaction is

$$\begin{aligned}
 V(\mathbf{r}_1, \mathbf{r}_2) = & t_0(1 + x_0 P_\sigma)\delta(\mathbf{r}) \\
 & + \frac{1}{2}t_1(1 + x_1 P_\sigma)[\mathbf{P}^2\delta(\mathbf{r}) + \delta(\mathbf{r})\mathbf{P}^2] \\
 & + t_2(1 + x_2 P_\sigma)\mathbf{P}' \cdot \delta(\mathbf{r})\mathbf{P} \\
 & + \frac{1}{6}t_3(1 + x_3 P_\sigma)[\rho(\mathbf{R})]^\sigma \delta(\mathbf{r}) \\
 & + iW_0\sigma \cdot [\mathbf{P}' \times \delta(\mathbf{r})\mathbf{P}], \tag{1}
 \end{aligned}$$

where $\mathbf{r} = \mathbf{r}_1 - \mathbf{r}_2$ is the relative coordinate of the two particles and $\mathbf{R} = (\mathbf{r}_1 + \mathbf{r}_2)/2$ the center-of-mass coordinate. $\mathbf{P} = (\nabla_1 - \nabla_2)/2i$ is the relative momentum acting on the right, and \mathbf{P}' its conjugate acting on the left. $P_\sigma = (1 + \sigma_1 \cdot \sigma_2)/2$ is the spin-exchange operator.

The force parameters are t_i and x_i , the power σ of the density dependence, and the spin-orbit strength W_0 . As already mentioned, the last parameter will be adjusted phenomenologically in some specific nucleus. As for the σ parameter, it is difficult to extract in a unique way just from nuclear matter bulk properties. In the literature, several classes of Skyrme forces are characterized by the value of σ , the most common values being 1/6, 1/3, and 1. Since we do not have enough constraints from BHF calculations of nuclear matter to determine all the

free parameters, we choose to adopt in this work $\sigma = 1/6$ and to concentrate on finding the remaining parameters.

The basic inputs of this work are the results of the BHF self-energy which includes the core polarization term [called in the literature the extended BHF approximation (EBHF) [12]] and the EOS with two- and three-body forces [8]. The procedure to determine the force parameters proceeds through three main steps. The first step concerns the fit of the nucleon effective mass in symmetric and nonsymmetric nuclear matter. This enables one to find the values of two important combinations Θ_s and Θ_v of t_1, t_2, x_1, x_2 . In the second step, we look at the energy per particle in symmetric and nonsymmetric nuclear matter as a function of total density and neutron-proton asymmetry. The fit of these quantities determines several families of (t_0, t_3, x_0, x_3) parameters. In the last step, we use the constraints imposed by the value of the G_0 Landau parameter and by a combination of parameters governing the surface properties of finite nuclei. In this way, the remaining parameters t_1, t_2, x_1, x_2 are uniquely determined for each parameter family since we already know the values of Θ_s and Θ_v . Because the fit of BHF bulk properties has been supplemented with the surface condition, one may hope that the parameter sets thus obtained could describe finite nuclei reasonably well.

A. Effective masses

In symmetric nuclear matter, the isoscalar effective mass of a nucleon has the following expression (here and in the rest of this paper we follow the same notations as in Ref. [4]):

$$\frac{m_s^*}{m} = \left(1 + \frac{m}{8\hbar^2} \rho \Theta_s \right)^{-1}, \quad (2)$$

where $\Theta_s = [3t_1 + (5 + 4x_2)t_2]$. One can also define an isovector effective mass as

$$\frac{m_v^*}{m} = \left(1 + \frac{m}{4\hbar^2} \rho \Theta_v \right)^{-1}, \quad (3)$$

where $\Theta_v = t_1(x_1 + 2) + t_2(x_2 + 2)$. In asymmetric nuclear matter with an asymmetry parameter $\beta = (N - Z)/A$, the nucleon effective mass is

$$\frac{m_q^*}{m} = \left(1 + \frac{m}{8\hbar^2} \rho \Theta_s - \frac{m}{8\hbar^2} q(2\Theta_v - \Theta_s)\beta \rho \right)^{-1}, \quad (4)$$

with $q = 1$ for neutrons and $q = -1$ for protons.

To obtain Θ_s , we fit the values of the nucleon effective mass calculated in symmetric nuclear matter in the EBHF approximation [12] with the three-body force effects included. The fit is illustrated in Fig. 1, and the resulting value from the fit is $\Theta_s = 400.8 \text{ MeV fm}^5$. Next, we can determine Θ_v by fitting m_q^*/m calculated in asymmetric nuclear matter. The fits are shown in Fig. 2, and the corresponding value of Θ_v is 356.4 MeV fm^5 . Actually, the fits of m_q^*/m remain good beyond $\beta = 0.4$.

At this point, we can already make an interesting observation. Some Skyrme parametrizations of the literature predict that for a fixed density, the proton and neutron effective masses are, respectively, an increasing and decreasing function of

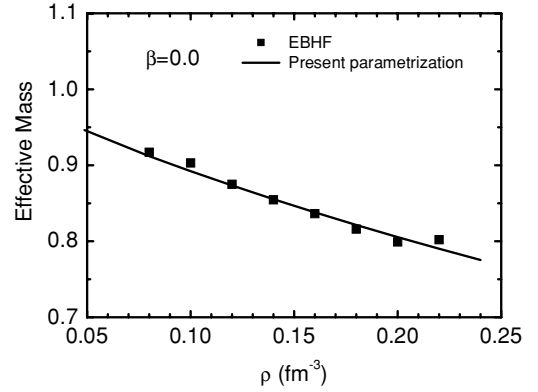


FIG. 1. Nucleon effective mass m^*/m in symmetric nuclear matter.

the asymmetry parameter β [14]. This behavior is opposite to that predicted by EBHF calculations [15]. In Fig. 3, we show a comparison of effective masses calculated with the parameter set SLy4 [4] and with our values of Θ_s and Θ_v . Thus, our Skyrme parametrization will differ from some usual parametrizations as far as the isospin splitting of effective masses is concerned. Recently, it was pointed out [17] that effective masses obtained in Dirac-Brueckner-Hartree-Fock have a similar behavior to that of EBHF, and opposite to that of the relativistic mean field (RMF) model. It must also be noted that if one includes the Fock terms in a relativistic Hartree-Fock description, the trend of the neutron-proton mass splitting becomes closer to that of the Dirac-Brueckner-Hartree-Fock

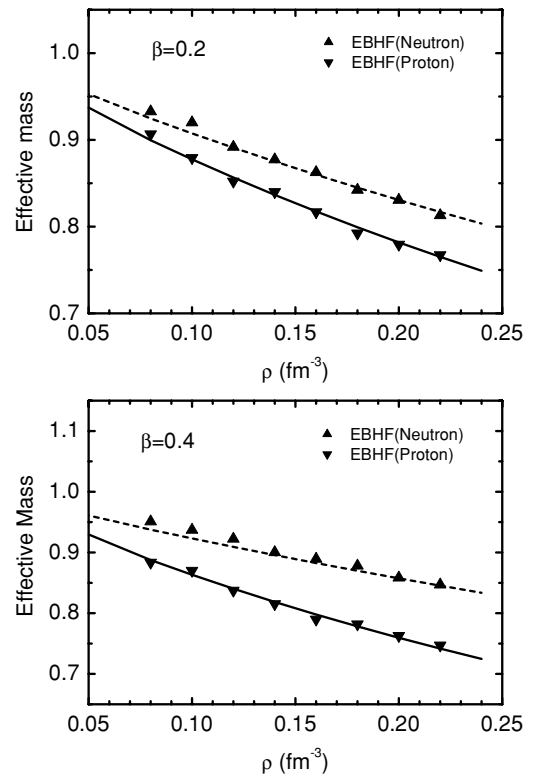


FIG. 2. Nucleon effective masses m_q^*/m in asymmetric nuclear matter, at two different asymmetries. Triangles are EBHF results, the lines are the fits.

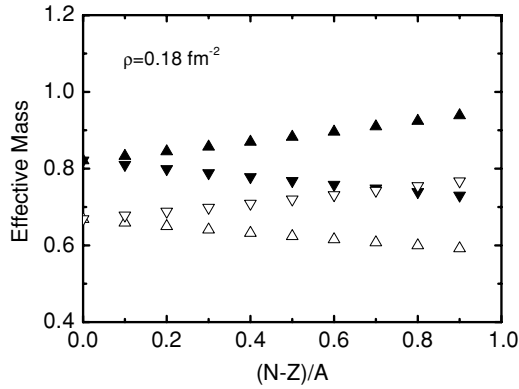


FIG. 3. Neutron (upward triangles) and proton (downward triangles) effective masses m^*/m calculated with SLy4 (in white) and with the present parametrization (in black).

and, therefore, the behavior of the RMF mass is due to the omission of exchange terms [27].

B. Energy per particle

In symmetric matter, the energy per particle has the following expression:

$$\begin{aligned} \frac{E}{A}(\rho) = & \frac{3\hbar^2}{10m} \left(\frac{3\pi^2}{2} \right)^{\frac{2}{3}} \rho^{\frac{5}{3}} + \frac{3}{8} t_0 \rho \\ & + \frac{3}{80} \Theta_s \left(\frac{3\pi^2}{2} \right)^{\frac{2}{3}} \rho^{\frac{5}{3}} + \frac{1}{16} t_3 \rho^{\sigma+1}. \end{aligned} \quad (5)$$

More generally, in asymmetric matter characterized by an asymmetry parameter β , the energy per particle is

$$\begin{aligned} \frac{E}{A}(\beta, \rho) = & \frac{3\hbar^2}{10m} \left(\frac{3\pi^2}{2} \right)^{\frac{2}{3}} \rho^{\frac{5}{3}} F_{\frac{5}{3}} + \frac{1}{8} t_0 \rho [3 - (2x_0 + 1)\beta^2] \\ & + \frac{1}{48} t_3 \rho^{\sigma+1} [3 - (2x_3 + 1)\beta^2] \\ & + \frac{3}{40} \left(\frac{3\pi^2}{2} \right)^{\frac{2}{3}} \rho^{\frac{5}{3}} \left[\Theta_v F_{\frac{5}{3}} + \frac{1}{2} (\Theta_s - 2\Theta_v) F_{\frac{5}{3}} \right], \end{aligned} \quad (6)$$

where $F_m(\beta) = \frac{1}{2}[(1 + \beta)^m + (1 - \beta)^m]$.

We first start with the case of symmetric matter. The fit of the BHF values of $\frac{E}{A}(\beta = 0, \rho)$ determines several possible values for the couple (t_0, t_3) . To limit the number of possible couples, we impose that the compression modulus K_∞ must be between 200 and 240 MeV. The optimal parameter sets we find have K_∞ around 210 MeV. As for ρ_0 , it is about 0.18 fm^{-3} in the BHF calculation with three-body force [8], a value somewhat larger than that usually adopted or predicted in Skyrme parametrizations. The consequence will be a general underestimation of radii in finite nuclei, as we shall see in Sec. IV.

For each (t_0, t_3) couple previously determined, we add the constraints of fitting $\frac{E}{A}(\beta \neq 0, \rho)$ as well as the symmetry energy $a_s(\rho)$ of infinite matter calculated in BHF. In terms of

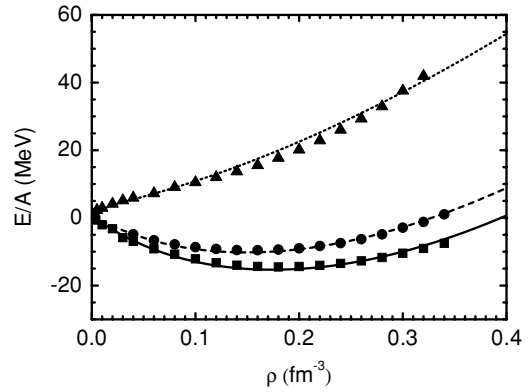


FIG. 4. Energy per particle as a function of density. Squares, dots, and triangles are BHF results for symmetric matter, $\beta = 0.4$ asymmetric matter, and neutron matter, respectively. Solid and dashed lines are results of the fit; dotted line is the extrapolation at $\beta = 1$.

Skyrme parameters, the symmetry energy $a_s(\rho)$ is

$$\begin{aligned} a_s(\rho) \equiv & \frac{1}{2} \left. \frac{\partial^2 (E/A)}{\partial \beta^2} \right|_{\beta=0} \\ = & \frac{1}{3} \frac{\hbar^2}{2m} \left(\frac{3\pi^2}{2} \right)^{\frac{2}{3}} \rho^{\frac{5}{3}} - \frac{1}{8} t_0 (2x_0 + 1) \rho \\ & - \frac{1}{24} \left(\frac{3\pi^2}{2} \right)^{\frac{2}{3}} (3\Theta_v - 2\Theta_s) \rho^{\frac{5}{3}} \\ & - \frac{1}{48} t_3 (2x_3 + 1) \rho^{\sigma+1}. \end{aligned} \quad (7)$$

In practice, we choose the EOS with $\beta = 0.4$ as the fitting object. In the fitting procedure, we set the symmetry energy at saturation density, $a_s(\rho_0) = 34 \text{ MeV}$ as a constraint for the full EOS of asymmetric nuclear matter. Thus, we obtain several possible solutions for (t_0, x_0, t_3, x_3) with t_0, t_3 already given by the symmetric matter fits and x_0, x_3 determined by nonsymmetric matter properties. Figures 4 and 5 display typical fits obtained in this way. Figure 4 shows the energies per particle in symmetric and $\beta = 0.4$ nonsymmetric nuclear matter, calculated in BHF and by the Skyrme procedure.

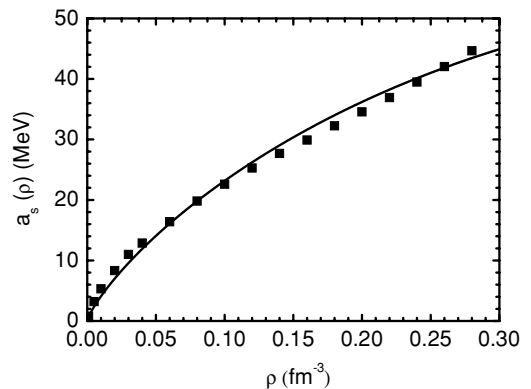


FIG. 5. Symmetry energy from BHF calculations (squares) and the present fit (solid curve).

The pure neutron matter case, which is not included in the fitting procedure, is also shown to demonstrate that the present Skyrme parametrizations describe reasonably well the BHF energies per particle in the whole range of β from 0 to 1 and for densities up to the highest BHF calculated values around 0.35 fm^{-3} . However, one can see that the Skyrme energy functional we adopted is not able to reproduce accurately the BHF EOS of pure neutron matter which exhibits an S-shaped behavior. This suggests that a change in the analytical structure of the energy functional would be necessary. In Fig. 5, we see the fit of BHF symmetry energy. The deviations observed in the neutron matter case in Fig. 4 reflect in the fit of the symmetry energy since the symmetry energy is calculated from the expression $a_s(\rho) = \frac{E}{A}(\rho, \beta = 1) - \frac{E}{A}(\rho, \beta = 0)$, and then a bad fit for the neutron matter EOS induces a bad fit for a_s .

To summarize, the bulk properties of nuclear matter have enabled us to determine several sets of (t_0, x_0, t_3, x_3) parameters and the values of the parameter combinations Θ_s and Θ_v for a fixed value $\sigma = 1/6$ of the density dependence. To complete the task, we determine the remaining parameters (t_1, x_1, t_2, x_2) in the next subsection.

C. Constraints from Landau parameters and finite nuclei

The bulk nuclear matter properties give only the two parameter combinations Θ_s and Θ_v . To proceed further, we can use some additional constraints from the Landau parameters corresponding to our reference EBHF calculation. These Landau parameters have been investigated in Ref. [25]. The two parameters F_0 and F'_0 are related to the compression modulus and symmetry energy, respectively, which are already incorporated into the preceding constraints. Then, only G_0 and G'_0 are left for providing two independent combinations of Skyrme parameters. Together with the Θ_s and Θ_v combinations, this would determine the four remaining parameters (t_1, x_1, t_2, x_2) . However, we prefer to use as constraint only G_0 , thereby giving us some freedom to better optimize the surface properties of finite nuclei. Indeed, the surface effects cannot be determined from infinite matter calculations, and we need to adjust these surface effects by performing Skyrme-Hartree-Fock (SHF) studies of some selected nuclei. The value of G_0 in EBHF [25] is 0.83 at $\rho_0 = 0.18 \text{ fm}^{-3}$. The parameter G_0 is expressed in the Skyrme parametrization [24] as

$$G_0 = N_0(2A + 2(3\pi^2\rho/2)^{\frac{2}{3}}B), \quad (8)$$

where N_0 is the level density at the Fermi surface and

$$A = -\frac{1}{4}t_0\left(\frac{1}{2} - x_0\right) - \frac{1}{24}t_3\left(\frac{1}{2} - x_3\right)\rho^\alpha, \quad (9)$$

$$B = -\frac{1}{8}t_1\left(\frac{1}{2} - x_1\right) + \frac{1}{8}t_2\left(\frac{1}{2} + x_2\right). \quad (10)$$

In the SHF energy functional, an important term governing surface properties of $N = Z$ systems is the term [4] $\alpha_s \nabla^2 \rho$ where $\alpha_s = [t_2(5 + 4x_2) - 9t_1]/32$. To determine the four parameters (t_1, x_1, t_2, x_2) satisfying the fixed values of Θ_s and Θ_v and also the spin-orbit parameter W_0 , we adopt the following procedure. We choose as reference nuclei the closed-shell and closed-subshell nuclei ^{16}O , $^{40,48}\text{Ca}$, $^{56,78}\text{Ni}$, ^{90}Zr , $^{100,132}\text{Sn}$ and ^{208}Pb . We vary α_s in a range of values

TABLE I. Skyrme parameter set and the corresponding bulk properties of infinite nuclear matter.

	LNS
t_0 (MeV fm ³)	-2484.97
t_1 (MeV fm ⁵)	266.735
t_2 (MeV fm ⁵)	-337.135
t_3 (MeV fm ^{3+3σ)}	14588.2
x_0	0.06277
x_1	0.65845
x_2	-0.95382
x_3	-0.03413
σ	0.16667
W_0 (MeV fm ⁵)	96.00
ρ_0 (fm ⁻³)	0.1746
E/A (MeV)	-15.32
K_∞ (MeV)	210.85
$\frac{m^*}{m}$ (isoscalar)	0.825
$\frac{m^*}{m}$ (isovector)	0.727
a_s (MeV)	33.4

similar to that of the usual Skyrme forces, and for each value we obtain a set of (t_1, x_1, t_2, x_2) with which we can perform a SHF calculation of the reference nuclei. The corresponding value of W_0 is obtained by adjusting the $p_{1/2}$ - $p_{3/2}$ proton splitting in ^{16}O . In this way, we can determine the set which gives the best overall results for binding energies and radii in the reference nuclei.

Table I summarizes the outcome of the fit. The full parameter set is called the LNS. In the lower part of Table I are shown the main bulk properties of nuclear matter calculated with LNS. Note that ρ_0 is larger and the saturation energy is slightly less negative than the empirical saturation point (0.16 fm^{-3} , -16.0 MeV). The consequence is that in finite nuclei, central densities will tend to be too large and radii become systematically underestimated.

IV. HF CALCULATIONS OF MAGIC NUCLEI

We now discuss the results of HF calculations of finite nuclei made with the LNS parametrization. The parameter set of Table I is supplemented with the two-body Coulomb force. The Coulomb exchange contributions are treated in the Slater approximation. The center-of-mass correction to the total energy is approximated in the standard way, keeping the one-body and dropping the two-body terms [28]. The HF equations are solved in the radial coordinate space, assuming spherical symmetry.

We choose to test the LNS parametrization on the following set of closed-shell and closed-subshell nuclei: ^{16}O , ^{40}Ca , ^{48}Ca , ^{56}Ni , ^{78}Ni , ^{90}Zr , ^{100}Sn , ^{132}Sn , and ^{208}Pb . The LNS force has not been fitted on finite nuclei and, therefore, one cannot expect a good quantitative description at the same level as purely phenomenological Skyrme forces. It is nevertheless interesting to compare its predictions with those of a commonly used force like the SLy4 interaction. In Fig. 6 are shown the relative deviations of charge radii and energies per particle calculated with LNS and SLy4. As for the binding energies, one can see

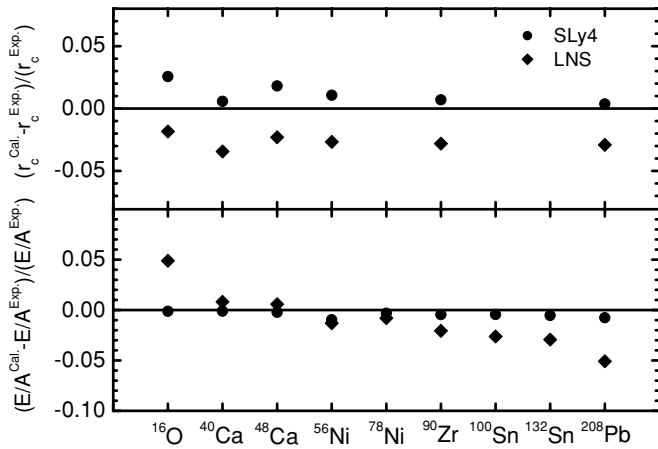


FIG. 6. The relative deviations of charge radii (upper panel) and energies per particle (lower panel) for the selected nuclei. The results calculated with LNS and SLy4 parametrizations are represented by diamonds and circles, respectively.

that LNS is doing reasonably well in the Ca and Ni regions, but it is underbinding somewhat ^{16}O and overbinding the medium and heavy nuclei, the discrepancies remaining within a 5% limit. This discrepancy is quite large if compared to the usual Skyrme predictions, but again the LNS force has not been fitted on finite nuclei. The SLy4 force is doing much better, of course, since it is adjusted on doubly magic nuclei. The deviations of the LNS energies can be attributed to the incorrect saturation point of the BHF equation of state, as well as to the lack of information concerning surface properties that one should fulfill. The charge radii of LNS exhibit a systematic behavior of underestimating the data by 2%–4%. This can be understood again as a consequence of the BHF saturation point being shifted toward a larger density. Then, the central density in nuclei calculated with LNS becomes larger than what it should be, and this reduces the spatial extension of nuclear densities. This is illustrated in Fig. 7, where we show the neutron and proton distributions in ^{208}Pb calculated with LNS and with SLy4.

Finally, we would like to comment on the spin-orbit component of the LNS parametrization since this is the only parameter that we could not relate to the EBHF calculation.

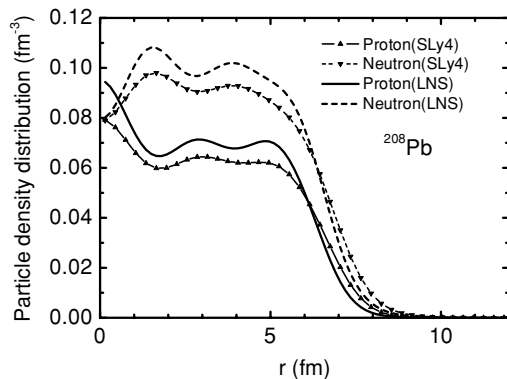


FIG. 7. Neutron and proton densities in ^{208}Pb , calculated with LNS and SLy4 parametrizations.

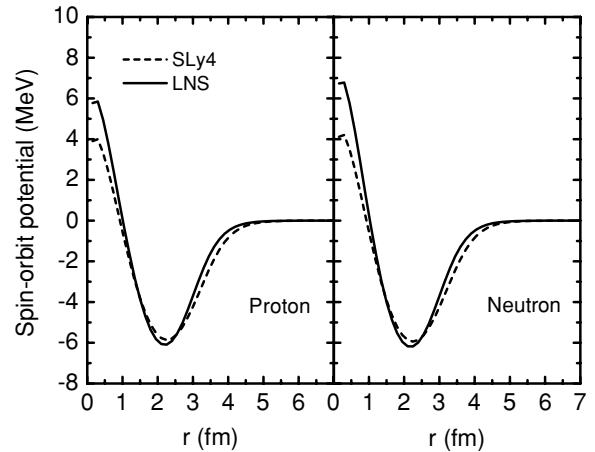


FIG. 8. Spin-orbit potentials in ^{16}O .

We have fitted it to reproduce the experimental $1p_{1/2}$ - $1p_{3/2}$ spin-orbit splitting of neutron and proton levels in ^{16}O . The value $W_0 = 96.0 \text{ MeV fm}^5$ that we find seems somewhat smaller than for other Skyrme forces where W_0 usually ranges from 105.0 to 130.0 MeV fm^5 . In Fig. 8, we show that the spin-orbit potentials in ^{16}O calculated with LNS and SLy4 are nevertheless very close and they must give the same spin-orbit splitting.

V. CONCLUSION

This work is the first step in deriving a Skyrme-type parametrization of an effective interaction suitable for Hartree-Fock calculations of finite as well as infinite systems. The starting point is the BHF calculations of infinite nuclear matter at different densities and neutron-proton asymmetries. These BHF studies include effects of three-body forces; consequently, the equation of state is much more satisfactory than with only two-body forces, and the saturation point becomes closer to the empirical point. This gives a good motivation for looking for a simple effective interaction—or energy density functional—whose parameters are determined by the BHF results.

We have paid special attention to the effective mass properties in order to get constraints on the velocity-dependent part of the effective force. The new Skyrme force obeys the BHF effective mass constraints, and hence the neutron and proton effective masses are, respectively, increasing and decreasing when increasing the asymmetry parameter β , a behavior not always obeyed by the usual Skyrme forces but consistent with empirical optical potential models [29]. The isospin splitting of effective mass in LNS force can be also probed in transport-model simulations of HIC with neutron-rich nuclei.

The LNS force that we have thus obtained looks quite promising in describing finite nuclei in the HF approximation. The deviations from the data remain at the level of a few percent for binding energies and radii. If the BHF results could be improved with respect to the equilibrium point of the equation of state, then the HF results of finite nuclei would most probably become much more satisfactory. In addition, the spin-orbit and pairing terms have still to be consistently

elaborated. In any case, it is highly desirable to establish a link between microscopic many-body theories carried out in infinite systems and phenomenological approaches for finite nuclei based on effective interactions. The present work is one step in that direction.

ACKNOWLEDGMENTS

This work was performed within the European Community project Asia-Europe Link in Nuclear Physics and Astrophysics, CN/ASIA-LINK/008(94791).

-
- [1] D. Vautherin and D. M. Brink, *Phys. Rev. C* **5**, 626 (1972).
 - [2] T. H. R. Skyrme, *Phil. Mag.* **1**, 1043 (1956); *Nucl. Phys.* **9**, 615 (1959).
 - [3] S. Goriely, M. Samyn, M. Bender, and J. M. Pearson, *Phys. Rev. C* **68**, 054325 (2003).
 - [4] E. Chabanat, P. Bonche, P. Haensel, J. Meyer, and R. Schaeffer, *Nucl. Phys.* **A627**, 710 (1997); **A635**, 231 (1998); **A643**, 441(E) (1998).
 - [5] R. B. Wiringa, V. Fiks, and A. Fabrocini, *Phys. Rev. C* **38**, 1010 (1988); R. B. Wiringa, *Rev. Mod. Phys.* **65**, 231 (1993).
 - [6] A. Akmal, V. R. Pandharipande, and D. G. Ravenhall, *Phys. Rev. C* **58**, 1804 (1998).
 - [7] H. Q. Song, M. Baldo, G. Giansiracusa, and U. Lombardo, *Phys. Rev. Lett.* **81**, 1584 (1998).
 - [8] W. Zuo, A. Lejeune, U. Lombardo, and J.-F. Mathiot, *Nucl. Phys.* **A706**, 418 (2002); *Eur. Phys. J. A* **14**, 469 (2002).
 - [9] J. W. Negele, *Phys. Rev. C* **1**, 1260 (1970).
 - [10] J. W. Negele and D. Vautherin, *Phys. Rev. C* **5**, 1472 (1972).
 - [11] M. Baldo, C. Maieron, P. Schuck, and X. Viñas, *Nucl. Phys.* **A736**, 241 (2004).
 - [12] W. Zuo, I. Bombaci, and U. Lombardo, *Phys. Rev. C* **60**, 024605 (1999).
 - [13] M. Baldo, *Nuclear Methods and the Nuclear Equation of State* (World Scientific, Singapore, 1999), p. 1.
 - [14] J. R. Stone, J. C. Miller, R. Konciewicz, P. D. Stevenson, and M. R. Strayer, *Phys. Rev. C* **68**, 034324 (2003).
 - [15] W. Zuo, L. G. Cao, B. A. Li, U. Lombardo, and C. W. Shen, *Phys. Rev. C* **72**, 014005 (2005).
 - [16] E. N. E. van Dalen, C. Fuchs, and A. Faessler, *Nucl. Phys.* **A744**, 227 (2004).
 - [17] Z. Y. Ma, J. Rong, B. Q. Chen, Z. Y. Zhu, and H. Q. Song, *Phys. Lett.* **B604**, 170 (2004).
 - [18] M. Di Toro, M. Colonna, and J. Rizzo, in NSCL/RIA Workshop on “Reaction Mechanisms for Rare Isotope Beams,” March 2005, AIP Proc. (to be published). nucl-th/0505013.
 - [19] I. Bombaci and U. Lombardo, *Phys. Rev. C* **44**, 1892 (1991).
 - [20] Bao-An Li, *Phys. Rev. C* **69**, 064602 (2004).
 - [21] A. M. Lane, *Nucl. Phys.* **35**, 676 (1962).
 - [22] Bao-An Li *et al.*, A Transport Model for Nuclear Reactions Induced by Radioactive Beams, in 2nd Argonne/MSU/JINA/INT RIA Workshop at MSU, March 9–12, 2005, AIP Proc. (to be published), arXiv/nucl-th/0504069.
 - [23] B. A. Brown, *Phys. Rev. Lett.* **85**, 5296 (2000).
 - [24] M. Bender, J. Dobaczewski, J. Engel, and W. Nazarewicz, *Phys. Rev. C* **65**, 054322 (2002).
 - [25] W. Zuo, C. Shen, and U. Lombardo, *Phys. Rev. C* **67**, 037301 (2003); C. Shen, U. Lombardo, N. Van Giai, and W. Zuo, *ibid.* **68**, 055802 (2003).
 - [26] T. Suzuki and H. Sakai, *Phys. Lett.* **B455**, 25 (1999).
 - [27] W. Long, N. Van Giai, and J. Meng, arXiv/nucl-th/0512086.
 - [28] M. Beiner, H. Flocard, N. Van Giai, and Ph. Quentin, *Nucl. Phys.* **A238**, 29 (1975).
 - [29] A. J. Koning and J. P. Delaroche, *Nucl. Phys.* **A713**, 231 (2003).